OXFORD

BJS Open, 2021, zrab061
DOI: 10.1093/bjsopen/zrab061
Original Article

Spatioregional assessment of the gut microbiota in experimental necrotizing pancreatitis

F. F. van den Berg [1,2,*], F. Hugenholtz[3], M. A. Boermeester[1], O. Zaborina [2] and J. C. Alverdy [2]

[1]Department of Surgery, Amsterdam Gastroenterology Endocrinology Metabolism, Amsterdam UMC, University of Amsterdam, Amsterdam, the Netherlands
[2]Department of Surgery, University of Chicago, Chicago, Illinois, USA
[3]Centre for Experimental and Molecular Medicine, Amsterdam UMC, University of Amsterdam, Amsterdam, the Netherlands

Correspondence to: Amsterdam UMC, location AMC, 1105 AZ Amsterdam, the Netherlands (e-mail: f.f.vandenberg@amsterdamumc.nl)

Abstract

Background: Infectious complications following experimental pancreatitis involve major disruptions in the gut microbiota. The aim of this study was to characterize this disruption by examining the spatioregional distribution in microbial community structure and function following experimental pancreatitis associated with pancreatic infection.

Methods: Mice were subjected to infusion of the pancreatic duct with either taurocholate to induce necrotizing pancreatitis or normal saline (control group). The spatial (lumen *versus* mucosa) and regional composition and function of the microbiota from the duodenum, ileum, caecum, colon, pancreas and blood were evaluated using 16S rRNA gene amplicon sequencing.

Results: Mice that developed necrotizing pancreatitis demonstrated a decrease in microbial richness and significantly altered microbiota in distal parts of the gastrointestinal tract, compared with controls. Among the most differentially increased taxa were the mucus-degrading *Akkermansia muciniphila*, and there was a decrease of butyrate-producing bacteria following pancreatitis. Application of the SourceTracker tool to the generated metadata indicated that the duodenum was the most probable source of bacteria that subsequently infected pancreatic tissue in this model. The functional prediction annotation using pathway analyses indicated a diminished capacity of the caecal microbiota to metabolize carbohydrate, and fatty and amino acids.

Discussion: The distal gut microbiota was significantly impacted in this model of experimental necrotizing pancreatitis. Data suggest that the duodenal microbiota might also play a role in bacterial translation and secondary infections.

Surgical Relevance

Intestinal bacteria are key disease modifiers in severe acute pancreatitis, especially when it comes to secondary infections such as pneumonia, bacteraemia and infected (peri-)pancreatic necrosis. Efficient and safe targeting of gut microbes as a way of prophylaxis warrants a deeper understanding of which bacteria in which intestinal compartment contribute to disease progression. This study investigated whether induction of necrotizing pancreatitis impacted the composition and function of the spatioregional gut microbiota in mice.

Necrotizing pancreatitis had a major effect on the microbiota distribution of the distal gastrointestinal tract with a reduction of butyrate-producing bacteria. The duodenum was identified as the main source of pancreatic infection in the model. These data suggest that microbial communities of both the upper and lower gastrointestinal tract might represent future targets for prophylaxis in patients with severe acute pancreatitis.

Introduction

Infection-related complications remain the most important determinant of the course, outcome and healthcare burden following severe acute pancreatitis. Although the intestinal tract is recognized to be the main site of origin of pathogens that cause infections during acute pancreatitis, the precise site and species that drive disease progression have been incompletely investigated[1–6]. Manipulations of the microbiome may fail to recognize off-target effects, such as when probiotics are used to replace lost microbiota or when broad-spectrum antibiotics are applied to eliminate emerging pathogens[7,8]. Empirical treatment with systemic meropenem, for example, prior to induction of experimental pancreatitis in mice, results in acceleration of mortality and increased infections, predominantly caused by gut-derived *Enterococcus gallinarum*[9]. Such findings may indicate that while certain pathogenic bacteria might require targeted elimination, others may need to be preserved in order to prevent loss of colonization resistance afforded by the normal microbiota. Evaluation of the gut microbiota following experimental pancreatitis has the potential to uncover which members of the microbiota are beneficial (such as butyrate-producers) and which are not, and, importantly, where such alterations occur[10,11].

It was hypothesized that region-specific changes in the gut microbiota could be defined that would predict subsequent

Received: April 11, 2021. **Accepted:** May 24, 2021

pancreatic infection in this model. The aims of this study were therefore to define the spatial (luminal *versus* mucosal) and regional (duodenum, ileum, caecum and colon) differences in microbial community structure and function using 16S rRNA gene amplicon sequencing in mice subjected to experimental pancreatitis and to assess how these changes related to pancreatic infection.

Methods

Ethical approval

All animal experiments were approved by the Institutional Animal Care and Use Committee of the University of Chicago (ACUP 72540).

Animal experiments

Six-week-old C57BL/6 mice were purchased (Charles River Laboratories International Inc., Wilmington, Massachusetts, USA) and housed under standard conditions (12 hours dark/light cycle) for 6 weeks before any study procedures were performed. Animals had *ad libitum* access to tap water and standard chow diet. Mice were anaesthetized with intraperitoneal ketamine (100 mg/kg) and xylazine (5 mg/kg) (Henry Schein Animal Health, Dublin, Ohio, USA). Before surgery, an injection of bupinorphrine (0.1 mg/kg) and meloxicam (1 mg/kg) was administered followed by postoperative injections of bupinorphrine every 12 hours for at least 48 hours. All procedures were performed under sterile conditions according to local guidelines and policies.

Murine model of acute biliary necrotizing pancreatitis

Necrotizing pancreatitis was induced by infusion of the pancreatic duct with taurocholate acid, as previously described[12]. This involved midline laparotomy, exposure of the posterior side of the duodenum and identification of the papilla of Vater followed by cannulation of the common bile duct for 2 mm and connection with PE-10 tubing (Fisher Scientific™, Waltham, Massachusetts, USA) attached to a syringe pump (Harvard apparatus, Holliston, Massachusetts, USA). The cannula was temporarily fixed with an 8/0 prolene suture, and a micro-clamp placed at the proximal hepatic duct. The pancreas was infused for 10 minutes with either 50 µl saline (controls, $n = 7$) or an equal volume of 4 per cent sodium taurocholate hydrate (pancreatitis, $n = 7$) with 1 per cent methyl-blue (Sigma-Aldrich, Saint-Louis, Missouri, USA). The cannula, micro-clamp and ligature were removed and the duodenal puncture closed, followed by routine wound closure. A group of mice that did not undergo surgery (untreated, $n = 5$) acted as a further comparator group.

All animals were sacrificed by carbon dioxide suffocation at either 24 or 72 hours following surgery. Sterile blood was collected by cardiac puncture. Pancreas and intestinal contents were aseptically removed and stored in saline with 10 per cent glycerol as cryopreservative at -80°C until analysis. Histology of pancreatic tissue was performed as previously described[13]. No technical replicates were used.

16s rRNA gene amplicon sequencing

Microbial DNA was extracted from pancreatic tissue and intestinal (duodenum, ileum, caecum, colon) tissues and contents using the MagAttract® PowerMicrobiome DNA/RNA KF kit and from blood using the DNeasy® Blood & Tissue kit (Qiagen, Germantown, Maryland, USA). Amplicons of the V4 region of the 16S rRNA gene were constructed using 515 F/806R primer pair, according to the Earth Microbiome Project protocols (EMP; http://www.earthmicrobiome.org/emp-standard-protocols/16s/). Gene amplicon sequencing was done on a MiSeq™ platform (Illumina, San Diego, California, USA) at the Argonne Sequencing Facility, generating 150 bp pair-end reads[14,15]. Decontaminating exact sequence variants (ESV) were removed using water control samples and the R package Decontam using the prevalence method with a threshold of 0.5[16]. Statistical analysis and visualization were done using R packages phyloseq and ggplot2[17,18]. A panel of butyrate-producers based on genus taxonomy was constructed as described previously[13,19]. The Inverse Simpson index was used as measure for alpha diversity which takes abundance into account. For beta diversity, the UniFrac distances were used to compare two communities based solely on the presence or absence of bacterial taxa (unweighted), or taking abundance into account (weighted). Differential abundance and microbial predictors were determined using R packages Deseq2 and Randomforest[20,21]. Investigation of Communities by Reconstruction of Unobserved States (PICRUSt) 2 tool that predicts functional aspects from 16S rRNA amplicon data using Kyoto Encyclopedia of Genes and Genomes (KEGG) and MetaCyC metabolic databases were used with QIIME2. Significant differences between predicted functional pathways were calculated using the R package Aldex2[13,22]. Blast was used for reads to determine a match at the species level[23]. The SourceTracker tool was designed to use 16S rRNA gene sequencing data to predict from which source a sample is determined[24]. Pancreatic and blood samples were used as 'sink', and the luminal and mucosal gut samples as 'source' using standard settings.

Untargeted gas chromatography–mass spectrometry metabolomics analysis

Following sacrifice at 24 hours following surgery, caecal content was collected, snap frozen and stored at -80°C until analysis. Ice-cold high-performance liquid chromatography (HPLC) grade water (100 µl) was added, homogenized and centrifuged at 16.000*g* for 20 minutes at 4°C. Supernatant was collected and 450 µl ice cold HPLC- grade methanol added, homogenized and centrifuged. The supernatants were combined and filtered through a 0.22 µm filter. Then 5 µl of 3 mg/ml myristic acid d27 (Sigma Aldrich, Saint-Louis, Missouri, USA) was added as internal control. The samples were evaporated in a Vacufuge® (Eppendorf, Hamburg, Germany) and the residue stored at -80°C.

Samples were derived by adding 50 µl of 20 mg/ml methoxyamine (Sigma) in pyridine. Samples were incubated at 37°C for 90 minutes in a shaking incubator. Next, 100 µl of MSTFA + 1 per cent TMC (Sigma) was added and incubated at 37°C for 30 minutes before analysis.

Samples were analysed using a high-resolution accurate mass 7200B QTOF gas chromatography–mass spectrometer (Agilent, Santa Clara, California) with a mass range 35–800, acquisition rate 6 spectra/s. Samples were randomized in batches of five, and injected at a 25 : 1 split ratio. A temperature programme of 70°C for 5 minutes was used, ramped at 5°C/min until 320°C, and held for 3 minutes. A blank sample containing solvent (pyridine) was run between each sample to clean the column of any residue. The chromatograms were processed (peak picking, definition of pseudospectra and annotation) using R (R Core Team, 2014) with the 'runGC' function of the metaMS package[25]. The resulting pseudospectra were annotated using the commercial Fiehn Gas Chromatography–Mass Spectrometry (GC/MS) Metabolomics RTL Library[26]. Features with matching factors 60 per cent or greater were positively identified.

Statistical analysis

Data were analysed using GraphPad Prism 8 (Graphpad Software, San Diego, California, USA) or R (R Core Team, 2014). Unless stated otherwise, results were expressed as mean(s.d.). Non-parametric Mann–Whitney or student *t* test was used to test statistical significance, depending on the distribution of normality. ANOVA was used to test significant differences between multiple groups. Benjamini–Hochberg correction was used for multiple comparison of groups. The Metaboanalyst 4.0 webserver module was used for the metabolome pathway analysis using normalized data and default settings with an FDR cut-off of 0.2[27].

Results

Histology of the pancreatic tissue of pancreatitis mice confirmed the presence of focal necrosis (Fig. S1a,b), in comparison with control mice that only showed mild oedema (Fig. S1c,d) and untreated mice (Fig. S1e,f). No mortality was observed prior to sacrifice.

The microbiota in all gut compartments in both mucus (Fig. 1a) and lumen (Fig. 1b) were affected by acute necrotizing pancreatitis (ANP) as seen by the distribution of ESVs. Overall, there was a relative loss of taxa in the pancreatitis group, as demonstrated by a decrease of richness in caecal ($P = 0.044$) and colonic mucosae ($P = 0.044$), but not in luminal samples (Fig. 1c). However, alpha diversity did not differ between groups (Fig. 1d) suggesting that mainly low-abundance taxa were affected.

Variance analysis of unweighted beta diversity showed that the centroids of the experimental groups significantly differed in the mucosal ileum ($R^2 = 0.162$, $P = 0.032$), mucosal and luminal caecum ($R^2 = 0.199$, $P = 0.024$ and $R^2 = 0.16$, $P = 0$ 0.043) and mucosal and luminal colon ($R^2 = 0.146$, $P = 0.008$ and $R^2 = 0.189$, $P = 0.008$ by PERMANOVA), but not in the duodenum (Fig. 1e). Weighted beta diversity did not differ significantly (Fig. 1f), again indicating that mostly low-abundance microbes were impacted. These differences were observed among both the luminal and mucosal microbiota. When comparing alpha and beta diversity of untreated and control mice, no major differences were observed (Fig. S2).

In comparing gut segments (Fig. S3) using the unweighted UniFrac measure, mucosal duodenal microbiota in animals with ANP closely resembled mucosal ileal microbiota ($P = 0.056$). In the control group mucosal duodenal and ileal microbiota differed markedly ($P = 0.001$) (Fig. S3).

To investigate possible involved bacterial pathways in the disease course of necrotizing pancreatitis, the authors next applied functional prediction on the microbiome data set (Fig. 2a)[28]. Prediction analysis demonstrated that multiple Kyoto Encyclopedia of Genes and Genomes (KEGG) pathways involved in carbohydrate, nucleotide and fatty acid metabolism were significantly downregulated in the caecal lumen following pancreatitis. Conversely, non-homologous end-joining was upregulated. MetaCyc pathway analysis additionally demonstrated upregulation of glucose, aromatic biogenic amine and 1,4-dihydroxy-2-napthoate metabolism. In the luminal colon, only degradation of purine nucleobases was decreased. There were no identifiable changes in regulatory pathways in the mucosal segments, nor in the duodenal or ileal luminal microbiota.

The metabolic profile of caecal luminal content in necrotizing pancreatitis and controls was further assessed with untargeted GC-MS metabolomics. Differential abundance analysis (Deseq2) demonstrated that two short-chain fatty acids, 2-hydroxybutyric acid and 5-aminovaleric acid, were decreased in pancreatitis (Fig. 2b). Amongst the increased metabolites were monosaccharides (D-mannose, D-lyxosylamine), phenolic acid (3-hydroxyphenylacetic acid), amino acid (L-threonine) and bile salt (cholic acid).

Analysis of differential abundant taxa of integrated luminal and mucosal segments (duodenum, ileum, caecum and colon) between the pancreatitis and control groups (Fig. S4) identified Verrucomicrobia, with its representative species *Akkermansia muciniphila*, as the sole phylum (Fig. 3a, $P < 0.050$) that differed between the groups, with an increase in the pancreatitis group. The phylum Firmicutes demonstrated an increase in the Erysipelotrichaeceae family, but a decrease in Lachnospiraceae in the pancreatitis group ($P < 0.050$). Although there was no difference in Proteobacteria, the phylum known to contain the majority of pathogens, bacteria from the genus *Escherichia/Shigella* were increased with pancreatitis ($P < 0.050$). Furthermore, there was both a decrease (mostly from the families Lachnospiraceae and Rumminococcaceae) and increase (genera *Butyricimonas* and *Ruminococcus*) of known butyrate-producing taxa ($P < 0.050$).

Investigation of the separate gut segments indicated no major shift in relative abundances of the four major phyla (Fig. S5a–d). Notably, Firmicutes : Bacteroidetes ratio demonstrated an approximately 50-fold decrease in the colonic mucosal (Fig. 3b), but not the luminal microbiota (Fig. S5e). Overall, there was a decrease of relative abundance of a panel of butyrate-producers in caecal mucosa (Fig. 3c). *Akkermansia muciniphila*, a mucus-degrading bacteria, was enriched in both the lumen and mucosa of caecum and colon (Fig. 3d and Fig. S5f).

Deseq2 analysis for differential abundance and a random forest classifier identified the genera that contributed the most in the prediction of the experimental groups. This analysis identified 43 decreased ESVs and 13 increased ESVs when combining gut segments of the groups ($P < 0.050$) (Fig. 4), with the majority overlapping in lumen and mucosa. In accordance with the alpha and beta diversity measures, the number of differential genera gradually increases along the gastrointestinal tract, with the majority found in the colon (47 genera), followed by caecum (29 genera), ileum (15 genera) and duodenum (15 genera) (Fig. S6a–d, $P < 0.050$). *Akkermansia muciniphila* was among the most increased abundant taxa in mucosa and lumen with both Deseq2 (Fig. 4) and random forest classifier (Fig. S7). *Escherichia/Shigella* was increased in the luminal compartment and mucosa of the caecum (Fig. S6c).

Sequencing of the 16S rRNA gene of pancreatic tissue after pancreatitis induction identified pathogens that translocate from the gastrointestinal tract to distant tissues. At the phylum and genus level, there were no major differences in relative abundances between the experimental and control group (Fig. 5a and Fig. S8).There were only two bacterial genera that were significantly overrepresented in pancreatic tissue based on Deseq2: *Proteus* and Lachnospiraceae_FCS02_group (Fig. 5b). The *Proteus* ESV in these samples had a 100 per cent identical match with *Proteus mirabilis*. Routine aerobic culture of pancreatic tissue following pancreatitis in this model revealed no *Proteus* species. Intestinal abundance of *Proteus* and Lachnospiraceae_FCS02_group were not significantly increased in the pancreatitis group. However, when comparing relative abundances between gut segments it was noted that *Proteus* abundance was highest in the duodenum, especially in mucosa (Fig. S9).

SourceTracker analysis indicated that the duodenum contributed 57 per cent to the disseminated bacteria, of which the majority were derived from the luminal compartment (Fig. 5c). In the control group 86 per cent could not be attributed to the

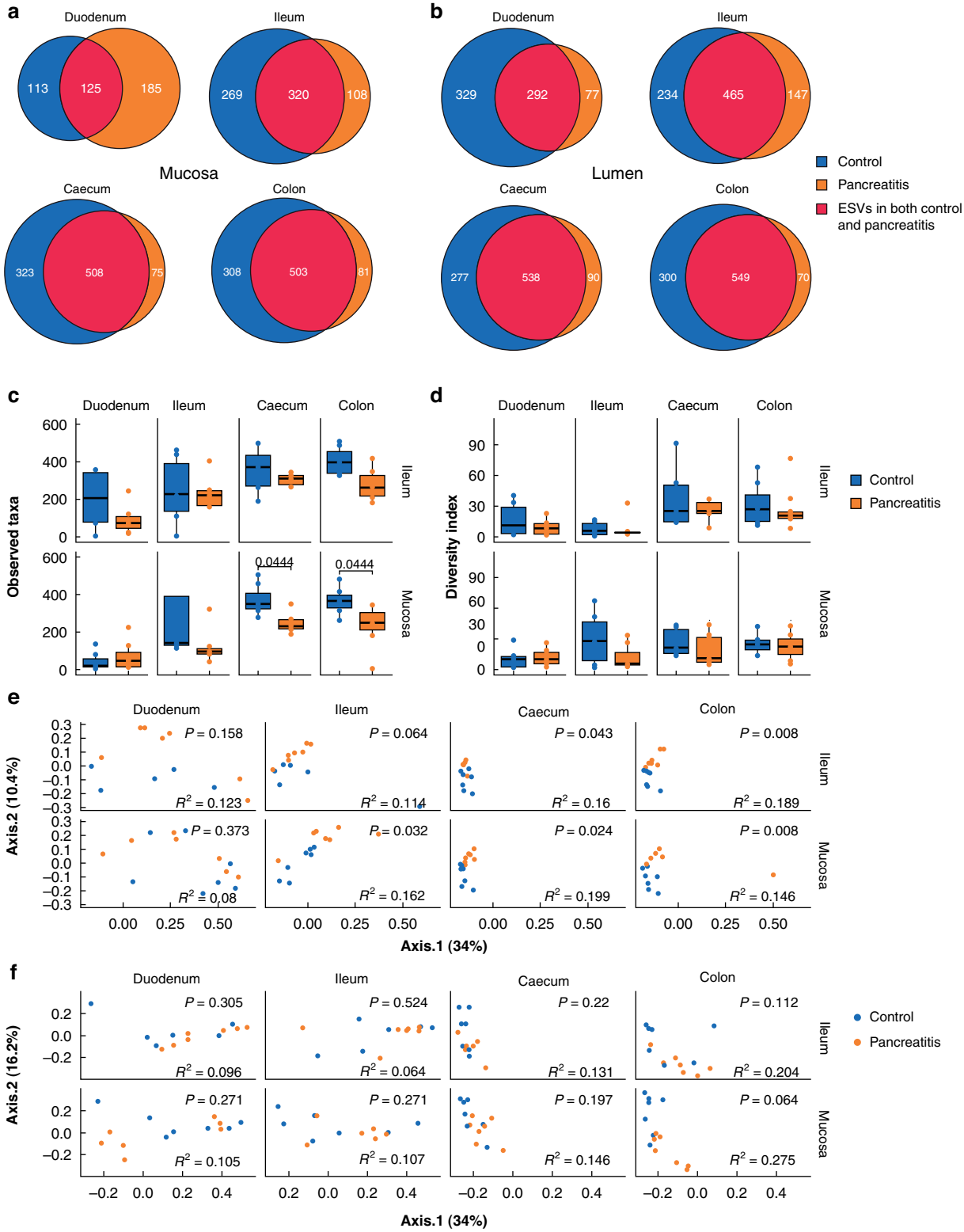

Fig. 1 Compositional analysis (16S rRNA gene analysis) of segmental lumen- and mucosa-associated microbiomes in acute necrotizing pancreatitis

Microbiota analysis of gut segments from mice with retrograde infusion of the pancreatic duct (pancreatitis) and saline-infused (control) mice ($n = 7$ per group). **a, b** Venn diagrams of exact sequence variants (ESVs) of gut segments from mucosa **a** and lumen **b**. **c** Richness (observed taxa) of luminal and mucosal gut segments. Richness was significantly decreased in caecum mucosa ($P = 0.044$, paired t-test with Benjamini-Hochberg correction) and colon mucosa ($p = 0.044$) of pancreatitis mice. **d** Alpha diversity of luminal and mucosal gut segments. No significant differences were found. **e, f** Beta diversity of luminal and mucosal gut segments measured by unweighted **e** and weighted **f** UniFrac. There were significant differences in ileum mucosa, caecum lumen and mucosa and colon lumen and mucosa for weighted UniFrac **e**, and in colon lumen and mucosa for unweighted UniFrac **f**. Beta diversity P and R^2 values based on PERMANOVA test with Benjamini-Hochberg correction. *$P < 0.050$, †$P < 0.010$

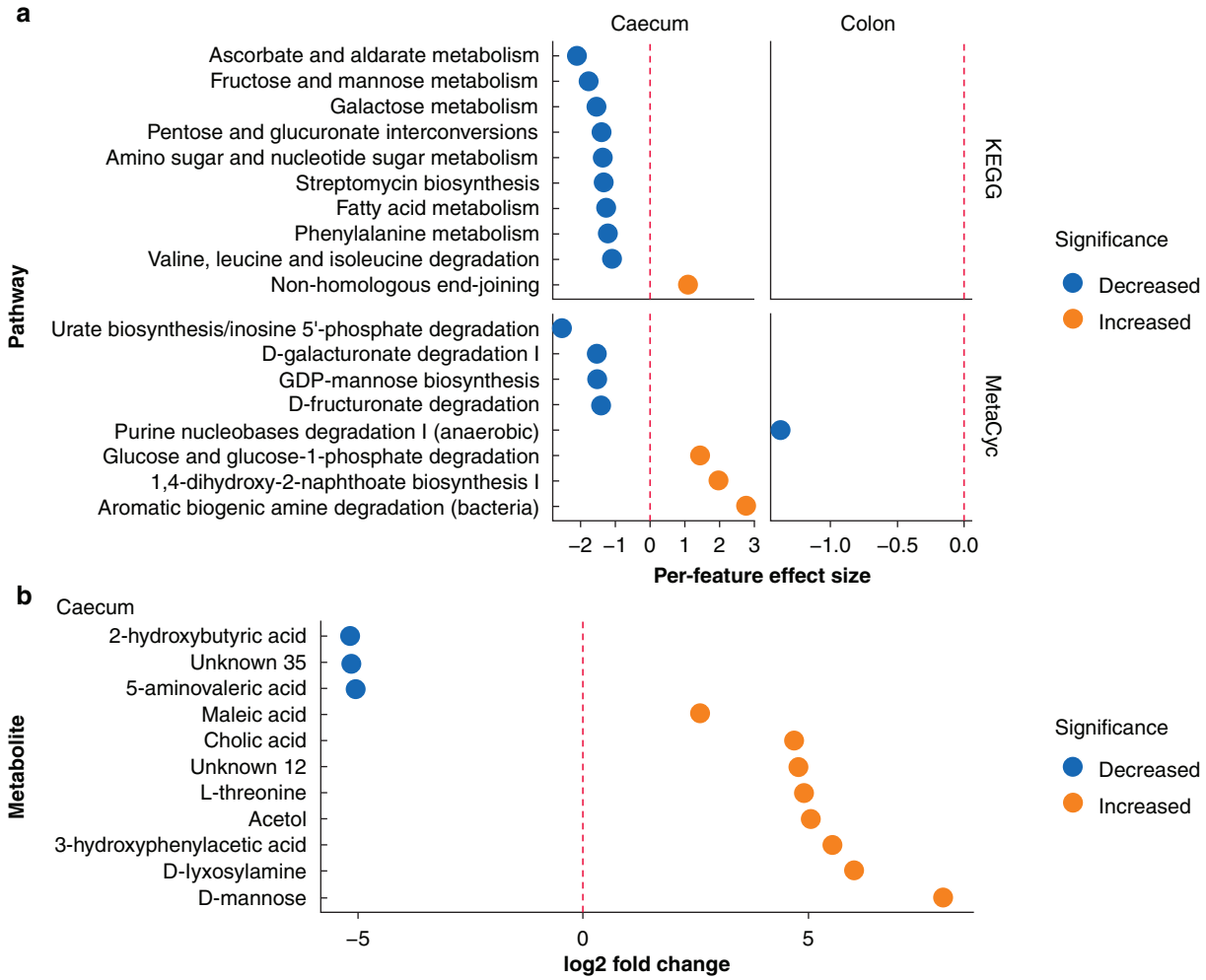

Fig. 2 Predicted up- and downregulated pathways and untargeted metabolomics of the gut microbiota following induction of necrotizing pancreatitis

a Prediction of differential regulated MetaCyc and Kyoto Encyclopedia of Genes and Genomes (KEGG pathways) of the microbiota using PICRUSt, followed by comparative analysing using Aldex was performed for pancreatitis mice compared with control mice. The per-feature effect size is shown for statistical differential pathways in caecum and colon lumen. Welch's *t* test (FDR $P < 0.100$) is used for statistical significance testing. **b** Untargeted GCMS metabolomics analysis of caecum content. Deseq2 analysis demonstrates differential caecal metabolites between pancreatitis and control mice. Log2 fold change is shown for statistical differential metabolites. Wald test (FDR $P < 0.100$) was used for statistical significance testing

gastrointestinal tract. In blood samples, only about 3 per cent of bacterial reads were predicted to have been derived from the gut segments in both control and pancreatitis animals (*Fig. 5d*). Although the relative abundance of *P. mirabilis* was highest in the duodenum compared with other gut segments, there was no difference in relative abundance of duodenal *P. mirabilis* between the pancreatitis and control group.

Discussion

Although bacterial overgrowth, impaired intestinal permeability and bacterial translocation to peripheral organs are widely recognized as hallmarks of disease progression in severe acute pancreatitis, the species involved in this process and their site of origin remain poorly understood. The present study investigated the biogeographical changes in microbial community composition, membership and function between different regions of the gastrointestinal tract in a clinically relevant animal model of necrotizing pancreatitis.

The present study demonstrated that necrotizing pancreatitis induced a shift within the lumen to mucosal-associated microbiota in some regions, with the mucosal microbiota appearing to display greater alterations in alpha (for mucosal caecum and colon) and beta diversity (for luminal ileum, caecum and colon). These differences appeared to be most pronounced in the colon. Although the mechanisms that govern this response remain to be identified, alterations in perfusion and oxygen tension as a result of the profound physiological perturbation that occurs during pancreatitis could be relevant[29]. A more complete description of the local physicochemical cues at precise sites within the spatial and regional contexts where microbiota reside during necrotizing pancreatitis is needed to elucidate these potential mechanisms fully.

The identification of *A. muciniphila*, a commensal mucus-degrading bacterium of the phylum Verrucomicrobia, in this model may be important, given increasing understanding into its role in intestinal health and gastrointestinal disorders[30]. *A. muciniphila* produces short-chain fatty acids, propionate and acetate, and works in synergy with downstream metabolizing bacteria that produce butyrate[31]. Experimental and clinical studies have shown that supplementation of live pasteurized strains of *A. muciniphila* and even purified membrane proteins have a beneficial effect on obesity and diabetes[32–35]. The role of *A. muciniphila*, which demonstrated a 20-fold increase in caecal mucosal

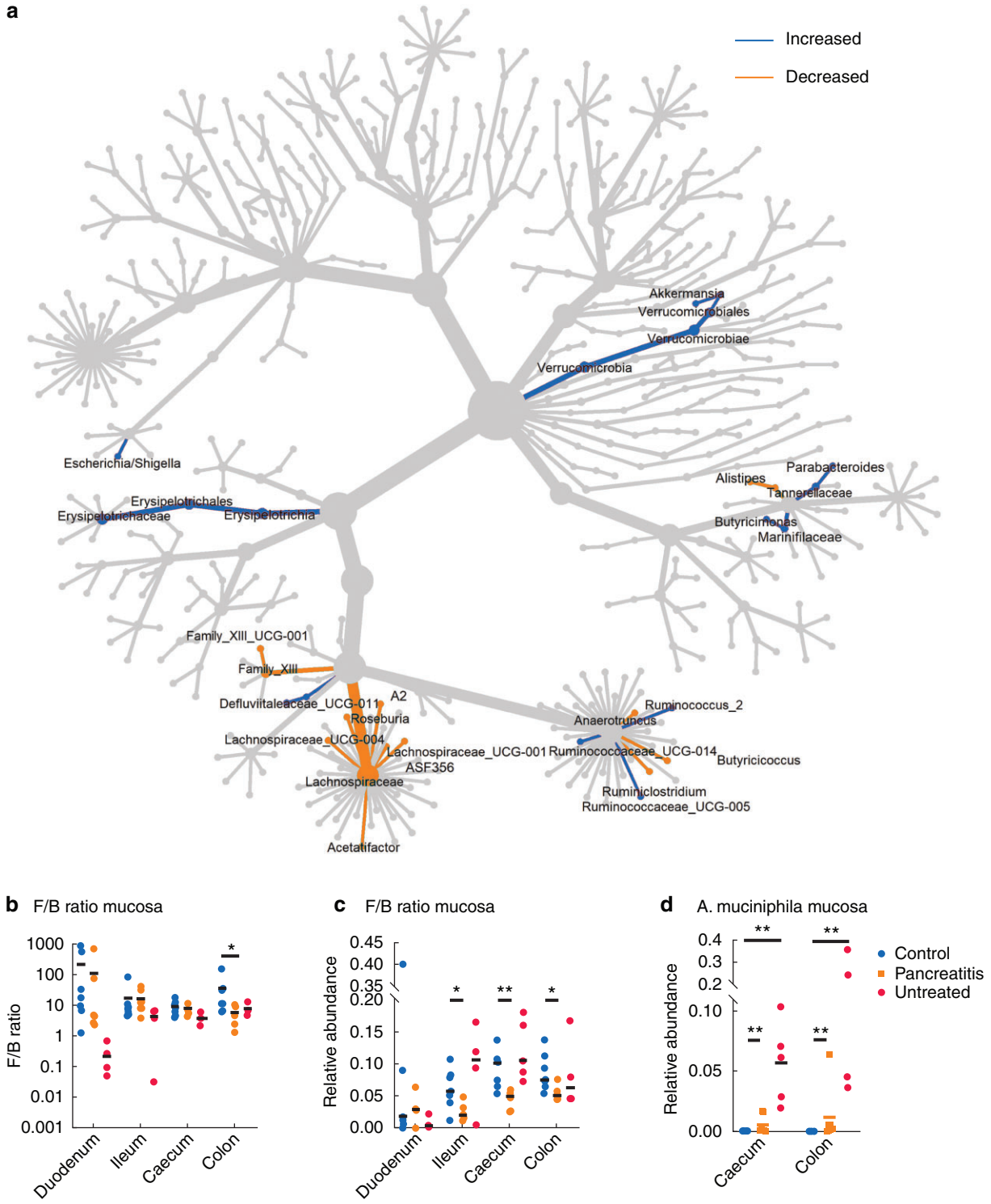

Fig. 3 Taxonomic tree and relative abundances in integrated gut segments of pancreatitis and control mice

a Taxonomic tree indicating significantly increased and decreased relative abundance of bacteria at different taxonomic levels of integrated luminal and mucosal segments (duodenum, ileum, caecum and colon) in pancreatitis group compared with controls ($P < 0.05$ by Kruskall–Wallis test with FDR correction). **b** Firmicutes/bacteroidetes (F/B) ratio of gut segments. F/B ratio is decreased in colon mucosa of pancreatitis mice ($P = 0.018$). **c** Relative abundance of butyrate-producers in caecum mucosa is decreased in the pancreatitis group ($P = 0.004$). **d** Relative abundance of *Akkermansia muciniphila* demonstrates an increase in mucosal caecum ($P = 0.003$) and colon ($P = 0.010$) in the pancreatitis group compared with the control group. *P* values based on Mann–Whitney test. *$P < 0.050$, †$P < 0.010$

samples and a 100-fold increase in the colonic mucosa at 72 hours after induction of necrotizing pancreatitis, remains to be clarified. It is possible that a bloom of mucus-degrading bacteria, such as *A. muciniphila*, may play a part in the known mucosal damage and altered intestinal integrity that develops in clinical and experimental pancreatitis[36,37]. In line with previous work[1,3,4,38,39] an increase of the *Escherichia/Shigella* genus in some gut compartments was noticed, implying a potential pathogenic role in this model of necrotizing pancreatitis. The majority of pathogens cultured in infected pancreatic collections (among

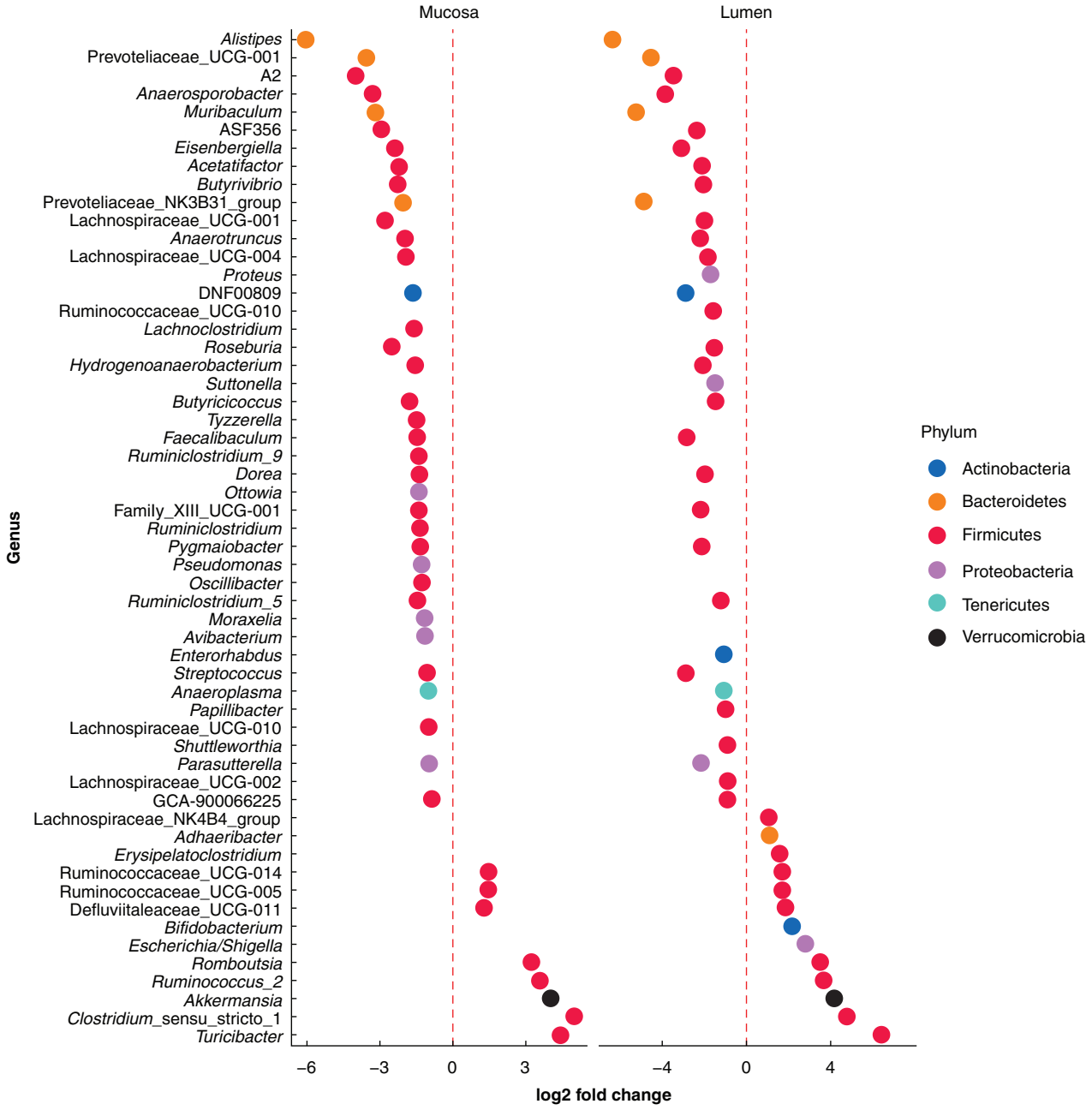

Fig. 4 Microbiome differential abundance analysis

Differential abundance of genera in mucosa and lumen of combined gut segments is tested using Deseq2. Colours indicate phylum. Wald-test is used for statistical significance ($P < 0.050$)

others *Escherichia coli* and *P. mirabilis*) are known gut inhabitants that are thought to translocate and cause (extra-) pancreatic infections[40,41]. There were no major differences in the pancreatic microbiome between pancreatitis and control mice, indicating that the majority of these taxa were either representations of a native pancreatic microbiome (if one exists), the results of intrinsic contamination of the DNA isolation or sequencing methods (despite computational decontamination) or as a result of the surgical procedure. Pancreatic over-representation of *Proteus mirabilis*, a facultative anaerobic Gram-negative pathogen frequently cultured in experimental and human infected necrotizing pancreatitis[42], might be the result of bacterial translation. One explanation why *P. mirabilis* was not cultured is that it was unable to survive and proliferate in the pancreatic tissue in this model. The high abundance of *Proteus* in the duodenum compared with levels in the distal gastrointestinal tract adds support to this.

A major finding in the present study was the implication that the pancreatic duct may be a route of infection from the duodenum which acts as a reservoir of potential invading pathogens. In contrast to other studies[43–46], the use of the SourceTracker tool pointed towards the duodenum as the most likely origin of pancreatic infection in this model. Other studies have demonstrated that bacteria can migrate to the pancreas of healthy mice within 30 minutes following their administration, suggesting that infection occurs proximally, perhaps directly via the pancreatic duct[47]. In this specific model, it is accepted that surgical trauma (laparotomy and cannulation) followed by inflammation (taurocholate

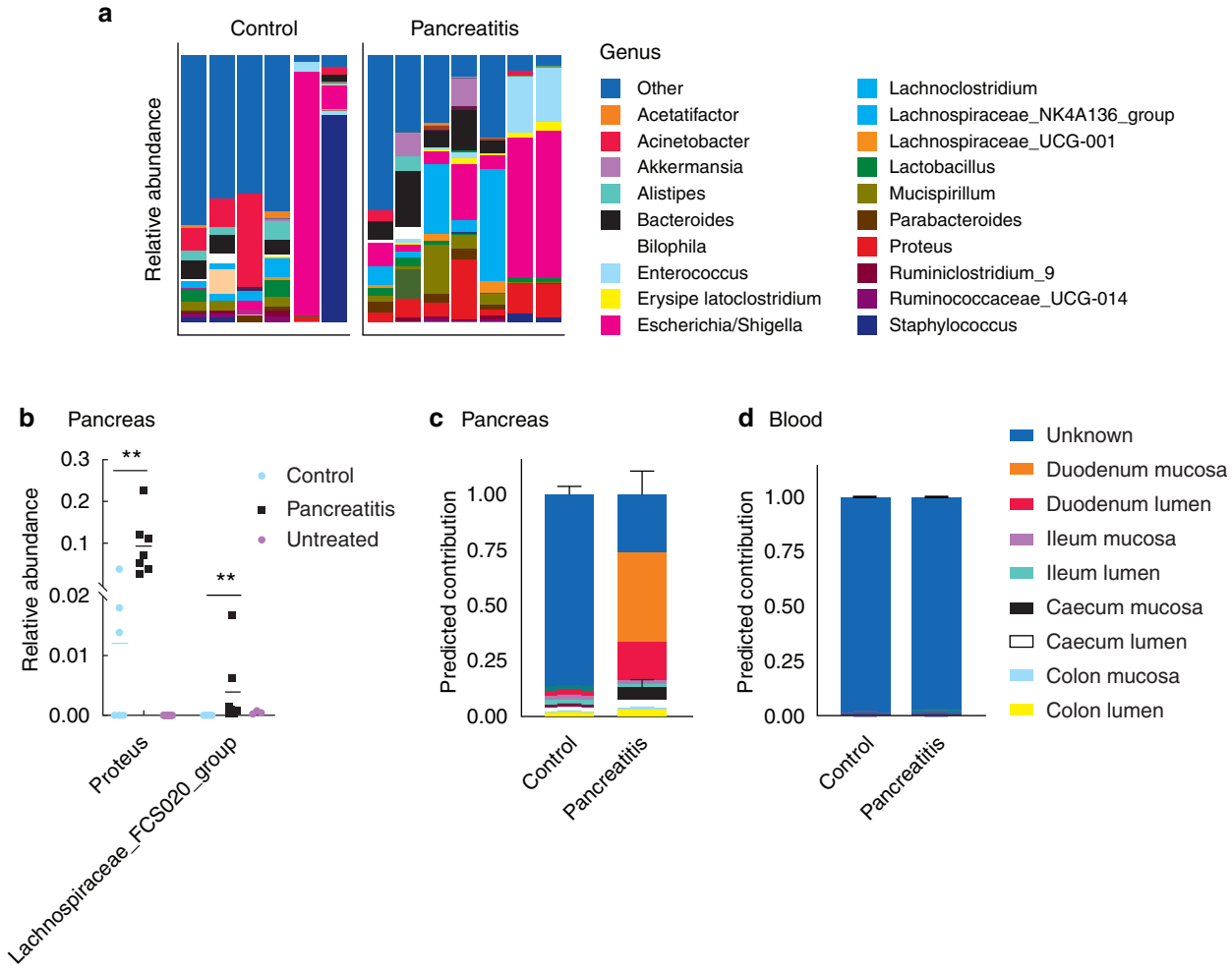

Fig. 5 Gut origin of bacteria disseminating to the pancreas during pancreatitis

a Relative abundance (16S rRNA gene analysis) at the genus level in pancreas tissue from pancreatitis and control mice. **b** Relative abundance of *Proteus* ($P = 0.003$) and Lachnospiraceae_FCS020_group ($P = 0.001$) were increased in pancreatitis mice, compared with levels in control mice. **c, d** SourceTracker was used to predict the contribution of different gut segments to the microbiota in the pancreas **c** and blood **d**. Mean and 95 per cent confidence intervals of predicted contribution are shown. In the pancreas, the majority was predicted to be contributed by the duodenal mucosa (40 per cent), followed by the duodenal lumen (approximately 17 per cent). The other gut segments contribution varied from 1 to 6 per cent. In the control group, only approximately 14 per cent in total was predicted to be contributed to the gut with even distribution among the segments. In blood, 3 per cent in total was predicted to be derived from the gut in both control and pancreatitis mice. *P* values based on Mann–Whitney test. *$P < 0.010$.

infusion) could lead to more contamination compared with trauma without subsequent inflammation (saline-infused control group).

There was discrepancy in terms of the gut regions where microbiota changes were most pronounced (caecum and colon), and the likely source of pancreatic infection in the present model (duodenum). This might reflect duodenal overgrowth with downstream microbes due to decreased intestinal motility. The timing of microbiota sampling might also be relevant. Duodenal microbiota changes that preceded pancreatic infections might have occurred before 72 hours.

In general, results from the present study were complementary to similar studies in this area[1,2,4,48] and parallel findings in patients with acute pancreatitis[4,6,39,49–51]. *Table 1* shows taxa from human studies that were significantly over- and under-represented in patients with acute pancreatitis compared with healthy subjects. Although previous studies use culture methods to describe the consequences of acute pancreatitis on the gut microbiome, genetic approaches reveal a much greater depth and breadth of changes in microbiota composition and function[4,51]. Transfer of human intestinal microbiota samples from patients with a specific disease process to germ-free mice is a powerful tool to link the microbiota to a specific disease phenotype[52]. While there are many limitations to the findings in the present study that do not allow a causal link to be established between duodenal microbiota and those that have migrated to the pancreatic tissues, the findings are compelling. Genetic sequencing of both faeces and saliva (which might better represent the upper gastrointestinal microbiota) or even endoscopy-acquired samples could test this hypothesis in the clinical situation. While marker gene sequencing has proved useful in characterizing the composition of microbial communities, functional output and ability to distinguish between ESVs is limited. Further studies using metagenomics and metatranscriptomics (whole genome/transcriptome shotgun-sequencing) and integrated analyses will need to be performed to extend these initial observations and provide a more detailed understanding of how the microbiota are altered within the complex environment of the gut, both regionally and spatially, when the host is exposed to the complex physiological disturbances that typically characterize acute pancreatitis.

Table 1 Microbiota changes from human studies with acute pancreatitis

Study	Tan *et al.* 2015[50]	Li *et al.* 2018[49]	Zhang *et al.* 2018[51]	Zhu *et al.* 2019[4]	Van den Berg *et al.* 2021[6]	Yu *et al.* 2021[39]
Sample	Faeces	Blood	Faeces	Faeces	Faeces	Rectal swab
Taxa						
G *Acinetobacter*		↓				
P Actinobacteria		↓				
G *Anaerococcus*		↓				
G *Bacteroides*		↑				
P Bacteroidetes		↑	↑	↓		
G *Bifidobacterium*	↑	↓		↓		
G *Blautia*				↓		
G *Burkholderia*		↓				
G Butyrate-producers					↓	
G *Brevundimonas*		↓				
G *Clostridium*		↑				
G *Corynebacterium*		↓				
G *Dietzia*		↓				
G Enterobacteriaceae	↑			↑		
G *Enterococcus*	↑			↑		↑
G *Escherichia/Shigella*				↑	↑	↑
G *Eubacterium*		↑				
G *Faecalibacterium*				↓		
P Firmicutes		↑	↓			
G *Flavobacterium*		↓	↓			
G *Fusobacterium*		↑				
G Lachnospiraceae				↓		
G *Lactococcus*		↓				
G *Legionella*		↓				
G *Paracoccus*		↑				
G *Prevotella*				↓		
G *Propionibacterium*		↓				
P Proteobacteria		↓	↑	↑	↑	
G *Pseudomonas*		↓				
G *Serratia*		↑				
G *Sphingobium*		↓				
G *Staphylococcus*		↑				
G *Stenotrophomonas*		↑				
G *Streptococcus*					↑	↑
G *Rhizobium*		↑				

G, Genus; P, Phylum. ↑ and ↓ represent, respectively, over- and under-representation of the taxa in pancreatitis *versus* healthy control subjects.

Acknowledgements

The authors thank Neil Gottel and Elle Hill, University of Chicago, for DNA isolation and library preparation and Mark Davids, Amsterdam UMC for help with the microbiota analysis. The generated data sets used for the analyses are available on reasonable request from the authors. O.Z. and J.C.A. are joint senior authors.

Disclosure. The authors report no conflict of interest.

Funding

This work was supported by the National Institutes of Health under Grant R01-GM062344-18 (J.C.A.); and the AMC Executive Board under grant AMC PhD Scholarship 2018 (F.B.).

Supplementary material

Supplementary material is available at *BJS Open* online.

References

1. Wan YD, Zhu RX, Bian ZZ, Pan XT. Improvement of gut microbiota by inhibition of P38 Mitogen-Activated Protein Kinase (MAPK) signaling pathway in rats with severe acute pancreatitis. *Med Sci Monit* 2019;**25**:4609–4616 doi:10.12659/MSM.914538.
2. Ye C, Liu L, Ma X, Tong H, Gao J, Tai Y *et al.* Obesity aggravates acute pancreatitis via damaging intestinal mucosal barrier and changing microbiota composition in rats. *Sci Rep* 2019;**9**:69 doi:10.1038/s41598-018-36266-7.
3. Zheng J, Lou L, Fan J, Huang C, Mei Q, Wu J *et al.* Commensal *Escherichia coli* aggravates acute necrotizing pancreatitis through targeting of intestinal epithelial cells. *Appl Enviro. Microbiol* 2019;**85**:e00059–00019 doi:10.1128/AEM.00059-19.
4. Zhu Y, He C, Li X, Cai Y, Hu J, Liao Y *et al.* Gut microbiota dysbiosis worsens the severity of acute pancreatitis in patients and mice. *J Gastroenterol* 2019;**54**:347–358 doi:10.1007/s00535-018-1529-0.
5. Li X, He C, Li N, Ding L, Chen HH, Wan J *et al.* The interplay between the gut microbiota and NLRP3 activation affects the severity of acute pancreatitis in mice. *Gut Microbes* 2020;1–16 doi:10.1080/19490976.2020.1770042.
6. van den Berg FF, van Dalen D, Hyoju SK, van Santvoort HC, Besselink MG, Wiersinga WJ *et al.* Western-type diet influences mortality from necrotising pancreatitis and demonstrates a central role for butyrate. *Gut* 2021;**70**:915–927 doi:10.1136/gutjnl-2019-320430.
7. Besselink MG, van Santvoort HC, Buskens E, Boermeester MA, van Goor H, Timmerman HM *et al.* Probiotic prophylaxis in predicted severe acute pancreatitis: a randomised, double-blind,

placebo-controlled trial. *Lancet* 2008;**371**:651–659 doi:10.1016/s0140-6736(08)60207-x.
8. Wittau M, Mayer B, Scheele J, Henne-Bruns D, Dellinger EP, Isenmann R *et al.* Systematic review and meta-analysis of antibiotic prophylaxis in severe acute pancreatitis. *Scand J Gastroenterol* 2011;**46**:261–270 doi:10.3109/00365521.2010.531486.
9. Soares FS, Amaral FC, Silva NLC, Valente MR, Santos LKR, Yamashiro LH *et al.* Antibiotic-induced pathobiont dissemination accelerates mortality in severe experimental pancreatitis. *Front Immunol* 2017;**8**:1890 doi:10.3389/fimmu.2017.01890.
10. Suez J, Elinav E. The path towards microbiome-based metabolite treatment. *Nat Microbiol* 2017;**2**:17075 doi:10.1038/nmicrobiol.2017.75.
11. Zhu W, Winter MG, Byndloss MX, Spiga L, Duerkop BA, Hughes ER *et al.* Precision editing of the gut microbiota ameliorates colitis. *Nature* 2018;**553**:208–211 doi:10.1038/nature25172.
12. Laukkarinen JM, Van Acker GJ, Weiss ER, Steer ML, Perides G. A mouse model of acute biliary pancreatitis induced by retrograde pancreatic duct infusion of Na-taurocholate. *Gut* 2007;**56**:1590–1598 doi:10.1136/gut.2007.124230.
13. van den Berg FF, van Dalen D, Hyoju SK, van Santvoort HC, Besselink MG, Wiersinga WJ *et al.* Western-type diet influences mortality from necrotising pancreatitis and demonstrates a central role for butyrate. *Gut* 2020 doi:10.1136/gutjnl-2019-320430.
14. Caporaso JG, Lauber CL, Walters WA, Berg-Lyons D, Huntley J, Fierer N *et al.* Ultra-high-throughput microbial community analysis on the Illumina HiSeq and MiSeq platforms. *ISME J* 2012;**6**:1621–1624 doi:10.1038/ismej.2012.8.
15. Caporaso JG, Lauber CL, Walters WA, Berg-Lyons D, Lozupone CA, Turnbaugh PJ *et al.* Global patterns of 16S rRNA diversity at a depth of millions of sequences per sample. *Proc Natl Acad Sci USA* 2011;**108**:4516–4522 doi:10.1073/pnas.1000080107.
16. Davis NM, Proctor DM, Holmes SP, Relman DA, Callahan BJ. Simple statistical identification and removal of contaminant sequences in marker-gene and metagenomics data. *Microbiome* 2018;**6**:226 doi:10.1186/s40168-018-0605-2.
17. McMurdie PJ, Holmes S. phyloseq: an R package for reproducible interactive analysis and graphics of microbiome census data. *PLoS One* 2013;**8**:e61217 doi:10.1371/journal.pone.0061217.
18. Wickham H. *ggplot2: Elegant Graphics for Data Analysis*. Springer Publishing Company, 2009.
19. Vital M, Karch A, Pieper DH. Colonic butyrate-producing communities in humans: an overview using omics data. *mSystems* 2017;**2** doi:10.1128/mSystems.00130-17.
20. Breiman L. Random Forests. *Mach Learn* 2001;**45**:5–32 doi:10.1023/a:1010933404324.
21. Love MI, Huber W, Anders S. Moderated estimation of fold change and dispersion for RNA-seq data with DESeq2. *Genome Biol* 2014;**15**:550 doi:10.1186/s13059-014-0550-8.
22. Fernandes AD, Macklaim JM, Linn TG, Reid G, Gloor GB. ANOVA-like differential expression (ALDEx) analysis for mixed population RNA-Seq. *PLoS One* 2013;**8**:e67019 doi:10.1371/journal.pone.0067019.
23. Altschul SF, Gish W, Miller W, Myers EW, Lipman DJ. Basic local alignment search tool. *J Mol Biol* 1990;**215**:403–410 doi:10.1016/s0022-2836(05)80360-2.
24. Knights D, Kuczynski J, Charlson ES, Zaneveld J, Mozer MC, Collman RG *et al.* Bayesian community-wide culture-independent microbial source tracking. *Nat Methods* 2011;**8**:761–763 doi:10.1038/nmeth.1650.
25. Wehrens R, Weingart G, Mattivi F. metaMS: an open-source pipeline for GC-MS-based untargeted metabolomics. *J Chromatogr B Analyt Technol Biomed Life Sci* 2014;**966**:109–116 doi:10.1016/j.jchromb.2014.02.051.
26. Kind T, Wohlgemuth G, Lee DY, Lu Y, Palazoglu M, Shahbaz S *et al.* FiehnLib: mass spectral and retention index libraries for metabolomics based on quadrupole and time-of-flight gas chromatography/mass spectrometry. *Anal Chem* 2009;**81**:10038–10048 doi:10.1021/ac9019522.
27. Xia J, Psychogios N, Young N, Wishart DS. MetaboAnalyst: a web server for metabolomic data analysis and interpretation. *Nucleic Acids Res* 2009;**37**:W652–660 doi:10.1093/nar/gkp356.
28. Douglas GM *et al.* PICRUSt2: an improved and extensible approach for metagenome inference. *bioRxiv* 2019;672295 doi:10.1101/672295.
29. Byndloss MX, Baumler AJ. The germ-organ theory of non-communicable diseases. *Nat Rev Microbiol* 2018;**16**:103–110 doi:10.1038/nrmicro.2017.158.
30. Geerlings SY, Kostopoulos I, de Vos WM, Belzer C. *Akkermansia muciniphila* in the human gastrointestinal tract: when, where, and how? *Microorganisms* 2018;**6** doi:10.3390/microorganisms6030075.
31. Belzer C, Chia LW, Aalvink S, Chamlagain B, Piironen V, Knol J *et al.* Microbial metabolic networks at the mucus layer lead to diet-independent butyrate and vitamin B12 production by intestinal symbionts. *mBio* 2017;**8** doi:10.1128/mBio.00770-17.
32. Dao MC, Everard A, Aron-Wisnewsky J, Sokolovska N, Prifti E, Verger EO *et al.*; MICRO-Obes Consortium. *Akkermansia muciniphila* and improved metabolic health during a dietary intervention in obesity: relationship with gut microbiome richness and ecology. *Gut* 2016;**65**:426–436 doi:10.1136/gutjnl-2014-308778.
33. Depommier C, Everard A, Druart C, Plovier H, Van Hul M, Vieira-Silva S *et al.* Supplementation with *Akkermansia muciniphila* in overweight and obese human volunteers: a proof-of-concept exploratory study. *Nat Med* 2019;**25**:1096–1103 doi:10.1038/s41591-019-0495-2.
34. Everard A, Belzer C, Geurts L, Ouwerkerk JP, Druart C, Bindels LB *et al.* Cross-talk between *Akkermansia muciniphila* and intestinal epithelium controls diet-induced obesity. *Proc Natl Acad Sci USA* 2013;**110**:9066–9071 doi:10.1073/pnas.1219451110.
35. Plovier H, Everard A, Druart C, Depommier C, Van Hul M, Geurts L *et al.* A purified membrane protein from *Akkermansia muciniphila* or the pasteurized bacterium improves metabolism in obese and diabetic mice. *Nat Med* 2017;**23**:107–113 doi:10.1038/nm.4236.
36. Fishman JE, Levy G, Alli V, Zheng X, Mole DJ, Deitch EA *et al.* The intestinal mucus layer is a critical component of the gut barrier that is damaged during acute pancreatitis. *Shock* 2014;**42**:264–270 doi:10.1097/SHK.0000000000000209.
37. Wu LM, Sankaran SJ, Plank LD, Windsor JA, Petrov MS. Meta-analysis of gut barrier dysfunction in patients with acute pancreatitis. *Br J Surg* 2014;**101**:1644–1656 doi:10.1002/bjs.9665.
38. Leveau P, Wang X, Soltesz V, Ihse I, Andersson R. Alterations in intestinal motility and microflora in experimental acute pancreatitis. *Int J Pancreatol* 1996;**20**:119–125 doi:10.1007/BF02825510.
39. Yu S, Xiong Y, Fu Y, Chen G, Zhu H, Mo X *et al.* Shotgun metagenomics reveals significant gut microbiome features in different grades of acute pancreatitis. *Microb Pathog* 2021;**154**:104849 doi:10.1016/j.micpath.2021.104849.
40. Besselink MG, van Santvoort HC, Boermeester MA, Nieuwenhuijs VB, van Goor H, Dejong CHC *et al.*; Dutch Acute Pancreatitis Study Group. Timing and impact of infections in acute pancreatitis. *Br J Surg* 2009;**96**:267–273 doi:10.1002/bjs.6447.

41. Widdison AL, Karanjia ND. Pancreatic infection complicating acute pancreatitis. *Br J Surg* 1993;**80**:148–154 doi:10.1002/bjs.1800800208.
42. Foitzik T, Mithöfer K, Ferraro MJ, Fernández-Del Castillo C, Lewandrowski KB, Rattner DW *et al.* Time course of bacterial infection of the pancreas and its relation to disease severity in a rodent model of acute necrotizing pancreatitis. *Ann Surg* 1994;**220**:193–198 doi:10.1097/00000658-199408000-00011.
43. Fritz S, Hackert T, Hartwig W, Rossmanith F, Strobel O, Schneider L *et al.* Bacterial translocation and infected pancreatic necrosis in acute necrotizing pancreatitis derives from small bowel rather than from colon. *Am J Surg* 2010;**200**:111–117 doi:10.1016/j.amjsurg.2009.08.019.
44. Gregg JA. Detection of bacterial infection of the pancreatic ducts in patients with pancreatitis and pancreatic cancer during endoscopic cannulation of the pancreatic duct. *Gastroenterology* 1977;**73**:1005–1007 doi:10.1016/S0016-5085(19)31848-7.
45. van Minnen LP, Nieuwenhuijs VB, de Bruijn MT, Verheem A, Visser MR, van Dijk JE *et al.* Effects of subtotal colectomy on bacterial translocation during experimental acute pancreatitis. *Pancreas* 2006;**32**:110–114 doi:10.1097/01.mpa.0000191650.24796.89.
46. Widdison AL, Alvarez C, Chang YB, Karanjia ND, Reber HA. Sources of pancreatic pathogens in acute pancreatitis in cats. *Pancreas* 1994;**9**:536–541 doi:10.1097/00006676-199407000-00019.
47. Pushalkar S, Hundeyin M, Daley D, Zambirinis CP, Kurz E, Mishra A *et al.* The pancreatic cancer microbiome promotes oncogenesis by induction of innate and adaptive immune suppression. *Cancer Discov* 2018;**8**:403–416 doi:10.1158/2159-8290.CD-17-1134 (2018).
48. Gerritsen J, Timmerman HM, Fuentes S, van Minnen LP, Panneman H, Konstantinov SR *et al.* Correlation between protection against sepsis by probiotic therapy and stimulation of a novel bacterial phylotype. *Appl Environ Microbiol* 2011;**77**:7749–7756 doi:10.1128/aem.05428-11.
49. Li Q, Wang C, Tang C, Zhao X, He Q, Li J *et al.* Identification and characterization of blood and neutrophil-associated microbiomes in patients with severe acute pancreatitis using next-generation sequencing. *Front Cell Infect Microbiol* 2018;**8**:5 doi:10.3389/fcimb.2018.00005.
50. Tan C, Ling Z, Huang Y, Cao Y, Liu Q, Cai T *et al.* Dysbiosis of intestinal microbiota associated with inflammation involved in the progression of acute pancreatitis. *Pancreas* 2015;**44**:868–875 doi:10.1097/mpa.0000000000000355.
51. Zhang XM, Zhang ZY, Zhang CH, Wu J, Wang YX, Zhang GX *et al.* Intestinal microbial community differs between acute pancreatitis patients and healthy volunteers. *Biomed Environ Sci* 2018;**31**:81–86 doi:10.3967/bes2018.010.
52. Berer K, Gerdes LA, Cekanaviciute E, Jia X, Xiao L, Xia Z *et al.* Gut microbiota from multiple sclerosis patients enables spontaneous autoimmune encephalomyelitis in mice. *Proc Natl Acad Sci USA* 2017;**114**:10719–10724 doi:10.1073/pnas.1711233114.